

Triboelectric Generators for Sustainable Reduction Leading to Nanoparticles and Nanoclusters

Vishal Kumar, Pillalamarri Srikrishnarka, Jyoti Sarita Mohanty, Murugesan Paulthangam Kannan, Ramamurthy Nagarajan, and Thalappil Pradeep*



Cite This: <https://doi.org/10.1021/acssuschemeng.1c01586>



Read Online

ACCESS |



Metrics & More



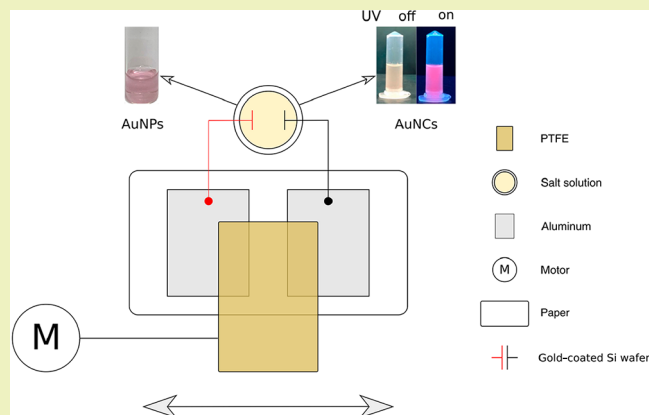
Article Recommendations



Supporting Information

ABSTRACT: In this letter, we demonstrate a sustainable, fast, and facile room temperature synthesis of plasmonic nanoparticles and luminescent nanoclusters of gold. The synthesis was performed using an affordable, easy to build, and robust triboelectric generator (TG). The electricity generated by the TG was transferred to the solution continuously to synthesize gold nanoclusters (AuNCs). The obtained AuNCs had extremely narrow size distributions with mean particle sizes of ~ 2 nm and showed bright pink luminescence under UV light. The approach was also extended to synthesize plasmonic gold nanoparticles (AuNPs). With this method, the synthesis time could be reduced from hours to several minutes without requiring any reducing agents. Tunability in size by simple variation of synthetic conditions and the consequent change in properties make this method usable for diverse applications.

KEYWORDS: Triboelectric generator, Gold nanoparticles, Gold nanoclusters



INTRODUCTION

Electrostatic charging or tribocharging plays an important role in a wide variety of fields.^{1–3} It has applications in areas such as photocopying,⁴ energy harvesting and power generation,⁵ synthesis of materials,⁶ sensors,⁷ air filtration,^{8,9} X-ray generation (triboluminescence) and imaging,¹⁰ and so forth.^{11,12} The history of triboelectricity dates back 300 BC to ancient Greek philosophers like Plato.¹³ The word “triboelectricity” was coined from two Greek words “tribo” meaning to rub and “elektron” (latter electricity) meaning amber.^{14,15} Tribocharging occurs when two materials are rubbed against each other and separated. A triboelectric series puts these materials based on the polarity and magnitude of charge generated. The farther materials are in the triboelectric series, the greater the amount of charge they acquire upon contact. The one high up in the series gets positively charged, while the other gets negatively charged. A triboelectric generator (TG)⁵ or paper generator¹⁶ uses triboelectric charging between materials and combines it with electrostatic induction to generate electricity. An increase in current from $\sim 0.6 \mu\text{A}$ ⁵ to $\sim 1.22 \text{ mA}$ ¹⁷ was recorded for TG, in less than a decade, which is an increase of more than 3 orders of magnitude. However, with these advancements, the complexity has also increased which could limit its broader applicability.

As bulk material reduces to the nanometer scale, its physical and chemical properties change drastically. These changes are

primarily a result of higher surface-to-volume ratios and changes in the electronic structure. One of the characteristic features of metal NPs is surface plasmon resonance (SPR), which is the collective oscillation of their conduction band electrons by the impinging light. This oscillation is responsible for the intense color of noble metal nanoparticles (NPs). NPs of this kind have sizes typically above 3 nm.¹⁸ Their physical and chemical properties make them ideal for labeling and detection of biomolecules,¹⁹ photodynamic therapy,²⁰ colorimetric sensing,²¹ surface-enhanced Raman spectroscopy (SERS),^{22,23} carriers for drug delivery,²⁴ catalysis,²⁵ and many more.²⁶

Upon further scaling down the size to the subnanometer regime, the particle size approaches the Fermi wavelength of electrons, and the quantum size effect becomes predominant. The quasi-continuous band transitions into molecule-like discrete energy states exhibiting drastically different optical and electronic properties compared to NPs and corresponding bulk materials.^{27,28} At this scale, the electronic properties are

Received: March 8, 2021

Revised: May 20, 2021

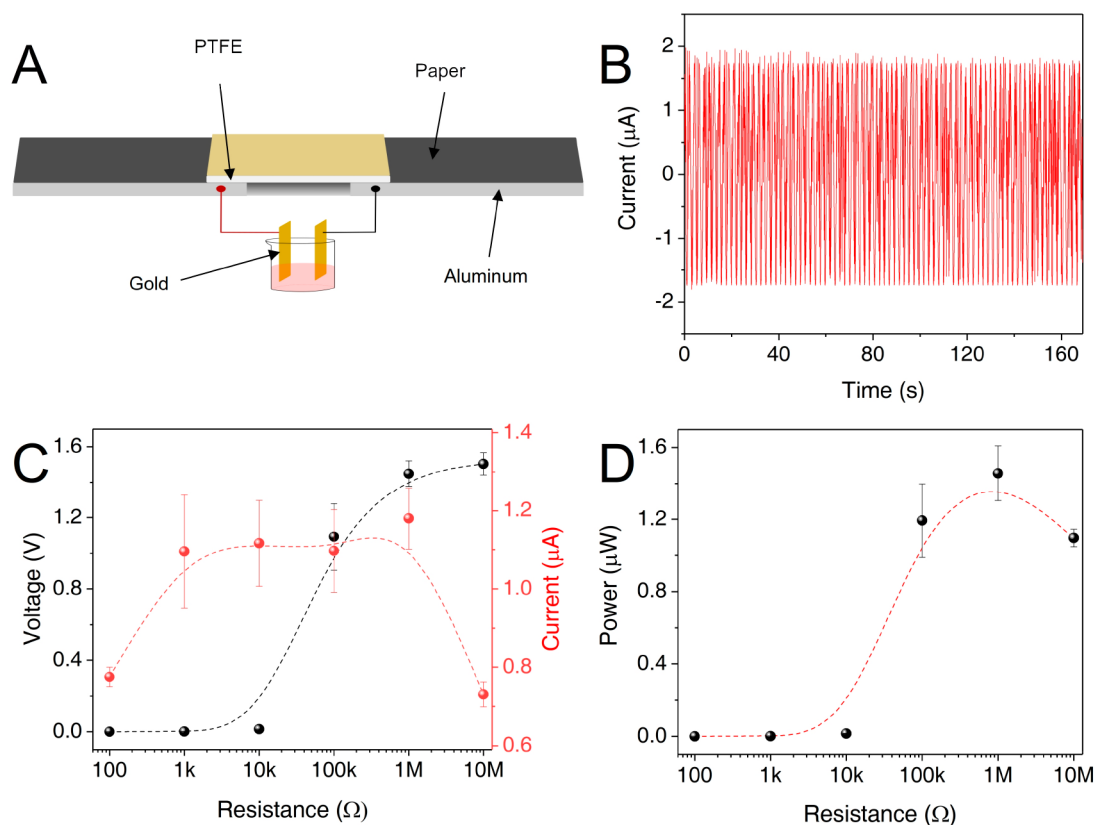


Figure 1. (A) Schematic of triboelectric generator setup for synthesis of NPs and NCs. (B) Short circuit current for the TG as a function of cycle of operations. (C) Output peak voltage and peak current. (D) Dependence of peak power with increasing resistance.

susceptible to the size and shape of the metal, and every atom counts in deciding the properties of such materials. This regime of the matter is called nanoclusters (NCs).²⁹ Properties vary significantly in the NPs and NCs regimes. For example, in the case of gold and silver, many NCs are visibly luminescent, while NPs have no observable luminescence. The fluorescence lifetimes and two-photon cross sections differ vastly for NCs and NPs. Moreover, the fluorescent emission of metal NCs can be tuned from infrared to UV regions by varying the core sizes.²⁷ These and several other unique properties have made metal NCs useful in areas such as bioimaging,³⁰ catalysis,^{31,32} chemical sensing,³³ and so forth.^{28,34,35} With time, several techniques to synthesize NPs and NCs have been developed.^{26,28,36} However, for NCs, the diversity possible makes it challenging to synthesize specific NCs.

In this letter, we demonstrated a simple and affordable means to synthesize AuNPs and AuNCs at room temperature using TG. Some early reports on the reduction of metal ions to NPs and bulk metal using triboelectric charging^{37–39} are available. Besides, one study demonstrated the synthesis of platinum NCs (PtNCs) using a triboelectric nanogenerator (TENG).⁴⁰ However, we did not find any reports concerning the synthesis of AuNCs using TG. Further, in a previous study,⁴⁰ the synthesis of PtNCs was performed on a catalytic surface which was also acting as an electrode. Moreover, the work exploits⁴⁰ the high surface activity of nanostructures like nanosheets. On the other hand, in our work, neither did we use any catalytic surface as an electrode nor exploit the high surface activity of nanostructures like nanosheets. The current TG requires a fewer number of components making it cost effective to assemble. The design is simple and easy to use.

With several simple modifications to the existing design,^{16,41} we significantly improved the robustness and longevity, enabling continuous synthesis of materials. The synthesis of NPs and NCs does not require any reducing agent, and capping agents were used to confine the size in the nanoscale regime. Typically, in wet chemical synthesis of NCs, sodium borohydride (NaBH_4) is used as a reducing agent, which is toxic and a health hazard. Since our synthesis procedure does not require any reducing agent, the synthesis process is green and sustainable. Moreover, the capping agent, 11-mercaptoundecanoic acid, used is nontoxic.

We discuss the synthesis of AuNPs, first followed by that of AuNCs. Initial results showed reduction, which was further established by spectroscopy and other techniques.

MATERIALS AND METHODS

Materials. Tetrachloroauric acid trihydrate ($\text{HAuCl}_4 \cdot 3\text{H}_2\text{O}$) was prepared starting from pure gold. The ligand, 11-mercaptoundecanoic acid (11-MUA), was purchased from Sigma-Aldrich. Glutathione reduced (GSH) was purchased from SRL. Mercaptosuccinic acid (MSA) was purchased from Aldrich. Sodium hydroxide (NaOH) pellets were purchased from Rankem. All the chemicals were used as received without further purification.

Instrumentation. UV–vis spectra were recorded using a PerkinElmer Lambda 25 instrument. High-resolution transmission electron microscopy (HRTEM) images were collected using a JEOL JEM 3010 (JEOL Japan) microscope. X-ray photoelectron spectroscopy (XPS) was carried out using an Omicron ESCA probe spectrometer with polychromatic Mg $K\alpha$ X-rays ($h\nu = 1253.6$ eV). Photoluminescence spectra were collected using a Jobin Yvon NanoLog instrument. The current and voltage measurements were performed using a Keithley 6514 system electrometer.

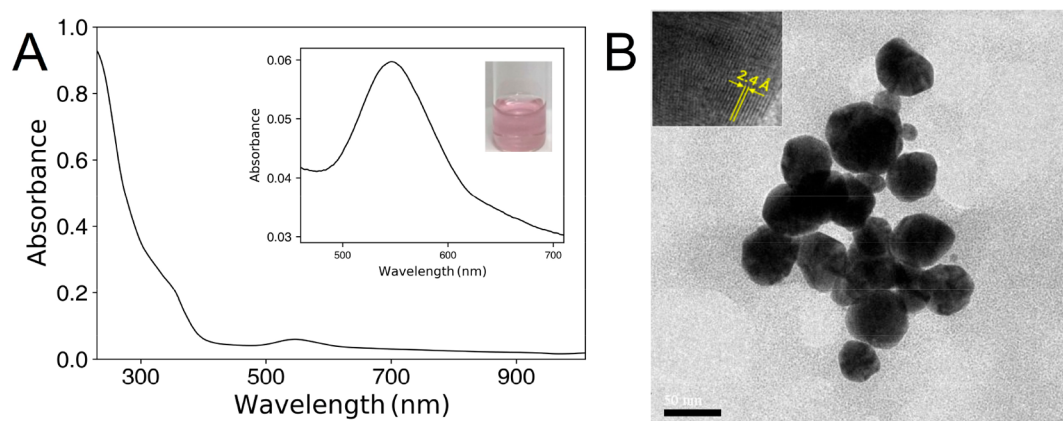


Figure 2. (A) UV-vis spectrum of triboelectrically synthesized MUA-AuNPs. Inset shows an expanded view showing the plasmonic peak at ~ 540 nm. (B) Photograph of the MUA-AuNPs (scale bar 50 nm). Inset shows lattice fringes.

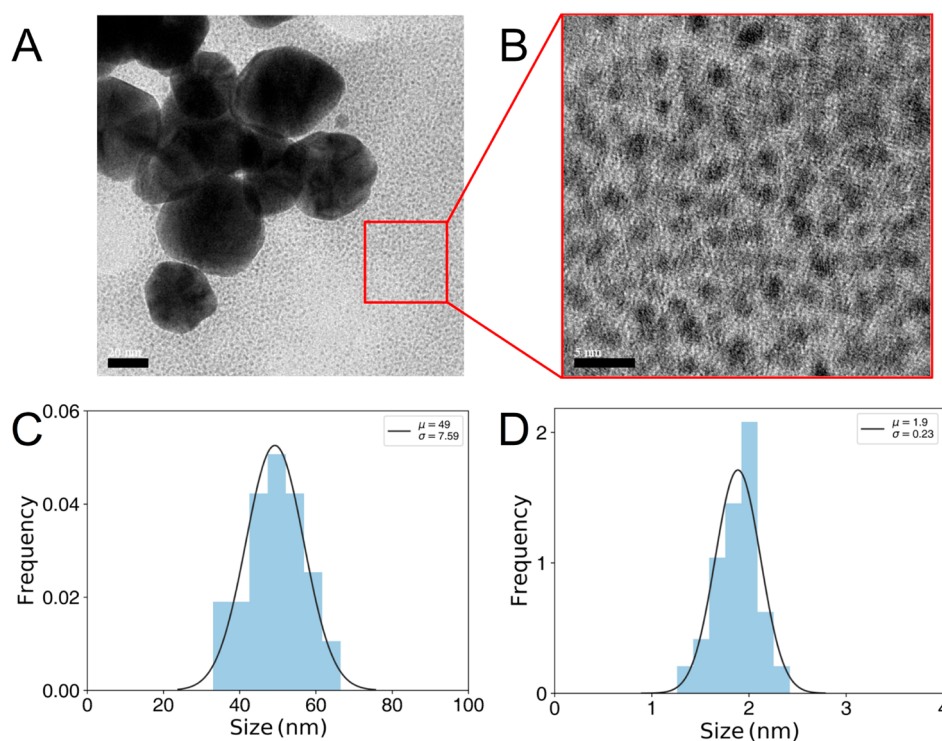


Figure 3. Two types of particles were observed in HRTEM: (A) bigger (scale bar 20 nm) and (B) smaller (scale bar 5 nm). (C, D) Size distributions for bigger and smaller MUA-AuNPs, respectively.

Design of TG. We chose the freestanding triboelectric layer mode⁴² to operate the TG in view of its ease of operation. Two aluminum (Al) tapes (thickness, $t \sim 0.05$ mm; area, $A = 13$ cm \times 7 cm) acting as electrodes were pasted on office paper ($t \sim 0.08$ mm) separated by 6 cm. In initial experiments, a PTFE ($t = 0.5$ mm; $A = 11$ cm \times 6 cm) sheet was driven over these electrodes gently with the help of a motor. The continuous rubbing of the PTFE on to the paper keeps it negatively charged. The charged PTFE, when moved over the electrodes, generates an electric current that could be transferred to a load. However, the continuous rubbing by the PTFE also causes scuffing of the Al, which significantly limits its long-term usability. To address this issue, we attached a paper on top of the electrodes and checked for the output current, as shown in Figure 1A. We did not observe any loss in current, and with this addition, we were able to increase the robustness and longevity of the system. The voltage and current of the TG were measured at various resistances, as shown in Figure 1C. The peak current stays almost the same up to 1 M Ω and

then began to drop as resistance increases. The peak voltage first rises and then started to saturate at ~ 1.6 V beyond 1 M Ω . The peak power for the TG was calculated from the peak voltage and peak current. The power rises with an increase in resistance, reaching a maximum at ~ 1 M Ω and then starts to fall off. We found that the TG works best when the distance between electrodes is of the order of the width of the electret (PTFE) (Figure S1) used for rubbing.⁴² To transfer the current into the solution, gold-coated silicon wafers were connected to the TG and dipped into the solution as shown in Figure 1A. Table S1 provides a brief comparison of the reported TENGs with our TG.

RESULTS AND DISCUSSION

Synthesis of AuNPs. For the synthesis of AuNPs, we used 11-MUA as a capping agent with HAuCl₄ as a precursor. The reaction volume was kept fixed to 2000 μ L for all the experiments. For this experiment, 750 μ L of 1 mM 11-MUA in

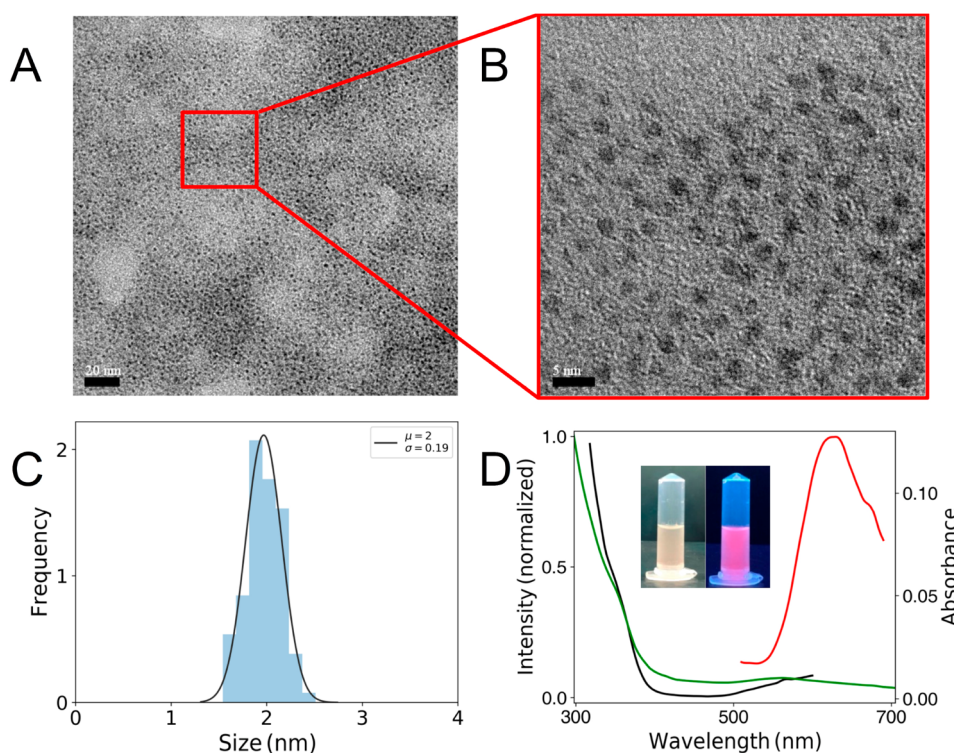


Figure 4. (A) HRTEM image of MUA-AuNCs (scale bar 20 nm). (B) Magnified TEM images (scale bar 5 nm). (C) MUA-AuNPs size distribution. (D) UV-vis absorption (green), fluorescence excitation (black, $\lambda_{em} = 623$ nm), and emission (red, $\lambda_{ex} = 355$ nm) spectra of MUA-AuNCs. The inset shows a photograph of MUA-AuNCs solution with UV light off (right) and on (left).

ethanol and 1250 μL of 10 mM of HAuCl_4 in distilled water were mixed. The solution was connected to the TG at room temperature with mild stirring, and electricity was applied for 30 min. During the synthesis, the current drawn by the solution does not show a significant decrease from the short circuit current, and the peak voltage of ~ 5.5 mV was recorded as shown in Figure S2. The solution was then centrifuged at 9000 rpm, and the precipitate was collected. The precipitate was washed five times in ethanol to remove any excess Au(I)-thiolate complexes and reactants present.⁴³ Finally, the precipitate was resuspended in water by adding a small amount of NaOH.^{44–46} NaOH was added because the basic pH allows the carboxyl groups to deprotonate and stabilize the NP dispersion through electrostatic repulsion.⁴⁴

A wine-red colored solution was obtained which showed an absorption peak at ~ 540 nm, indicating the presence of AuNPs. The spectrum also showed a broad shoulder peak centered near ~ 350 nm, as shown in Figure 2A. There is a slight shoulder in the red region, likely due to variations in particle morphologies. Nearly spherical particles of ~ 50 nm are seen in the TEM. The inset of Figure 2B shows a d spacing of ~ 0.24 nm, corresponding to the (111) plane of face-centered cubic Au. From the HRTEM, we observed particles with two kinds of distributions. The larger particles have average particle sizes of ~ 50 nm (Figure 3A,C), and smaller particles have average sizes of ~ 2 nm (Figure 3B,D).

Synthesis of AuNCs. The synthesis of AuNCs was carried out similarly to that of the AuNPs, except for the change in the reaction medium. The ligand, 11-MUA, is sparingly soluble in water but highly soluble in ethanol. So, to reduce turbidity, we chose ethanol as the reaction medium. We prepared 10 mM of HAuCl_4 in ethanol starting from a 330 mM aqueous solution

of HAuCl_4 . About 1 mM 11-MUA was prepared in ethanol. The solution was prepared by mixing reactants in the same volume as for the synthesis of AuNPs. After applying a current for 30 min, the solution was centrifuged at 9000 rpm. The obtained precipitate was washed several times in ethanol to remove any excess of Au(I)-thiolate complexes and reactants present. Finally, the precipitate was dispersed in water with NaOH or NH_4OH , to enhance solubility.⁴³ The solution showed bright luminescence under UV light. The HRTEM images (Figure 4A, B) showed uniform MUA-AuNCs of ~ 2 nm diameters. Figure 4D shows the UV-vis spectrum and fluorescence spectrum of the synthesized particles. The UV-vis spectrum showed an absorption at ~ 560 nm and a shoulder band at ~ 360 nm. A bright pink luminescence was obtained upon exposure to UV light. The fluorescence spectrum showed a strong emission peak at 623 nm upon excitation at 355 nm, which complies with the UV-vis spectrum. The characteristic feature of thiolate-protected gold clusters appears around 610 nm.⁴⁷ From the HRTEM images, we obtained a mean particle size of ~ 2 nm with a standard deviation, σ , of ~ 0.19 nm (Figure 4C). The XPS spectrum (Figure S4) showed a binding energy of 84.3 eV, corresponding to Au $4f_{7/2}$, taking the C 1s line of adventitious hydrocarbon at 284.8 eV as the reference. The binding energy is between 84.0 eV for Au(0) and 85.0 eV for Au(I), which indicates the presence of both Au(0) and Au(I) species in NC. AuNCs with thiolate protection is known to show the Au $4f_{7/2}$ feature around 84.45 eV.³³ The S $2p_{3/2}$ feature appears at 163.3 eV, as expected in the case of thiolate-protected clusters (Figure S5).

To further explore this process, we conducted experiments with water-soluble ligands, GSH and MSA. They were chosen as NPs made can form stable dispersions in water without the

use of a base. The gold solution with both GSH and MSA gave NPs upon applying triboelectricity. The formations of GSH-AuNPs and MSA-AuNPs were confirmed with UV-vis spectroscopy with plasmonic peaks at ~550 and ~560 nm, respectively (Figure S6).

CONCLUSION

We demonstrated a facile and fast technique for the synthesis of NPs and NCs using TG. The approach we devised is easy to perform and does not require any conventional reducing agent. Further, the TG used to carry out the synthesis requires a fewer number of components which makes it affordable and easy to build. With this technique, differently sized nanomaterials can be synthesized at room temperature. Several factors could affect the size of the synthesized particles. These include varying the voltage and current. One way to increase both the current and voltage is by using materials with high surface areas like electrospun fibers, which could significantly enhance the triboelectric charging. Other parameters of equal importance include the effect of the synthesis medium (its dielectric constant and dipole moment) and frequency of rubbing. Further, increasing the frequency of rubbing and/or enhancing surface area with micro- or nanostructuring results in an enhanced rate of charge transfer, thus increasing the yield of NPs and NCs. Using nanostructured surfaces for triboelectric charging typically increases the voltage by several folds (Table S1), which may affect particle synthesis, and it needs to be taken into account. Extending the method for the preparation of nanoparticles of other metals and alloys may be possible. The methodology developed is sustainable and simple.

ASSOCIATED CONTENT

Supporting Information

The Supporting Information is available free of charge at <https://pubs.acs.org/doi/10.1021/acssuschemeng.1c01586>.

Peak current at varying electrode distance, brief comparison of performance of published TENGs with our TG, XPS spectrum of MUA-AuNCs in Au 4f region, XPS spectrum of MUA-AuNCs in S 2p region current and voltage measurements for aqueous gold solution during synthesis of MUA-AuNPs, size distribution of MUA-AuNCs, current and voltage measurement for gold solution in ethanol during synthesis of MUA-AuNCs, and UV-vis spectra of aqueous GSH-AuNPs and MSA-AuNPs suspensions (PDF)

AUTHOR INFORMATION

Corresponding Author

Thalappil Pradeep – Department of Chemistry, DST Unit of Nanoscience (DST UNS) and Thematic Unit of Excellence (TUE), Indian Institute of Technology Madras, Chennai 600036, India; orcid.org/0000-0003-3174-534X; Email: pradeep@iitm.ac.in

Authors

Vishal Kumar – Department of Chemistry, DST Unit of Nanoscience (DST UNS) and Thematic Unit of Excellence (TUE) and Department of Chemical Engineering, Indian Institute of Technology Madras, Chennai 600036, India; orcid.org/0000-0002-2374-0568

Pillalamarri Srikrishnarka – Department of Chemistry, DST Unit of Nanoscience (DST UNS) and Thematic Unit of Excellence (TUE) and Department of Chemical Engineering, Indian Institute of Technology Madras, Chennai 600036, India; orcid.org/0000-0001-5187-6879

Jyoti Sarita Mohanty – Department of Chemistry, DST Unit of Nanoscience (DST UNS) and Thematic Unit of Excellence (TUE), Indian Institute of Technology Madras, Chennai 600036, India

Murugesan Paulthangam Kannan – Department of Chemistry, DST Unit of Nanoscience (DST UNS) and Thematic Unit of Excellence (TUE), Indian Institute of Technology Madras, Chennai 600036, India

Ramamurthy Nagarajan – Department of Chemical Engineering, Indian Institute of Technology Madras, Chennai 600036, India

Complete contact information is available at:

<https://pubs.acs.org/doi/10.1021/acssuschemeng.1c01586>

Notes

The authors declare no competing financial interest.

ACKNOWLEDGMENTS

We thank the Department of Science and Technology, Government of India, for continuously supporting our research program. V.K. and P.S. acknowledge institute graduate fellowships.

REFERENCES

- (1) Kok, J. F.; Renno, N. O. Electrostatics in Wind-Blown Sand. *Phys. Rev. Lett.* **2008**, *100* (1), 014501.
- (2) Steinpilz, T.; Joeris, K.; Jungmann, F.; Wolf, D.; Brendel, L.; Teiser, J.; Shinbrot, T.; Wurm, G. Electrical Charging Overcomes the Bouncing Barrier in Planet Formation. *Nat. Phys.* **2020**, *16* (2), 225–229.
- (3) Sayfidinov, K.; Cezan, S. D.; Baytekin, B.; Baytekin, H. T. Minimizing Friction, Wear, and Energy Losses by Eliminating Contact Charging. *Science Advances* **2018**, *4* (11), No. eaau3808.
- (4) Pai, D. M.; Springett, B. E. Physics of Electrophotography. *Rev. Mod. Phys.* **1993**, *65* (1), 163–211.
- (5) Fan, F. R.; Tian, Z. Q.; Lin Wang, Z. Flexible Triboelectric Generator. *Nano Energy* **2012**, *1* (2), 328–334.
- (6) Li, A.; Luo, Q.; Park, S.-J.; Cooks, R. G. Synthesis and Catalytic Reactions of Nanoparticles Formed by Electrospay Ionization of Coinage Metals. *Angew. Chem., Int. Ed.* **2014**, *53* (12), 3147–3150.
- (7) Yang, Y.; Zhu, G.; Zhang, H.; Chen, J.; Zhong, X.; Lin, Z.-H.; Su, Y.; Bai, P.; Wen, X.; Wang, Z. L. Triboelectric Nanogenerator for Harvesting Wind Energy and as Self-Powered Wind Vector Sensor System. *ACS Nano* **2013**, *7* (10), 9461–9468.
- (8) Liu, J.; Jiang, T.; Li, X.; Wang, Z. L. Triboelectric Filtering for Air Purification. *Nanotechnology* **2019**, *30* (29), 292001.
- (9) Srikrishnarka, P.; Kumar, V.; Ahuja, T.; Subramanian, V.; Selvam, A. K.; Bose, P.; Jenifer, S. K.; Mahendranath, A.; Ganayee, M. A.; Nagarajan, R.; Pradeep, T. Enhanced Capture of Particulate Matter by Molecularly Charged Electrospun Nanofibers. *ACS Sustainable Chem. Eng.* **2020**, *8* (21), 7762–7773.
- (10) Camara, C. G.; Escobar, J. V.; Hird, J. R.; Putterman, S. J. Correlation between Nanosecond X-Ray Flashes and Stick-Slip Friction in Peeling Tape. *Nature* **2008**, *455* (7216), 1089–1092.
- (11) Galembeck, F.; Burgo, T. A. L.; Balestrin, L. B. S.; Gouveia, R. F.; Silva, C. A.; Galembeck, A. Friction, Tribochemistry and Triboelectricity: Recent Progress and Perspectives. *RSC Adv.* **2014**, *4* (109), 64280–64298.
- (12) Nag, A.; Baksi, A.; Ghosh, J.; Kumar, V.; Bag, S.; Mondal, B.; Ahuja, T.; Pradeep, T. Tribochemical Degradation of Polytetrafluoro-

ethylene in Water and Generation of Nanoplastics. *ACS Sustainable Chem. Eng.* **2019**, *7* (21), 17554–17558.

(13) Lacks, D. J.; Shinbrot, T. Long-Standing and Unresolved Issues in Triboelectric Charging. *Nature Reviews Chemistry* **2019**, *3* (8), 465–476.

(14) Hummel, R. E. *Electrical Conduction in Metals and Alloys. In Electronic Properties of Materials*; Springer: New York, 2011; pp 79–114.

(15) Lacks, D. J.; Mohan Sankaran, R. Contact Electrification of Insulating Materials. *J. Phys. D: Appl. Phys.* **2011**, *44* (45), 453001.

(16) Karagozler, M. E.; Poupyrev, I.; Fedder, G. K.; Suzuki, Y. Paper Generators. In *Proceedings of the 26th Annual ACM Symposium on User Interface Software and Technology - UIST '13*; ACM Press: New York, 2013; pp 23–30.

(17) Chun, J.; Ye, B. U.; Lee, J. W.; Choi, D.; Kang, C. Y.; Kim, S. W.; Wang, Z. L.; Baik, J. M. Boosted Output Performance of Triboelectric Nanogenerator via Electric Double Layer Effect. *Nat. Commun.* **2016**, *7* (May), 1–9.

(18) Jin, R.; Zeng, C.; Zhou, M.; Chen, Y. Atomically Precise Colloidal Metal Nanoclusters and Nanoparticles: Fundamentals and Opportunities. *Chem. Rev.* **2016**, *116* (18), 10346–10413.

(19) Wilson, R. The Use of Gold Nanoparticles in Diagnostics and Detection. *Chem. Soc. Rev.* **2008**, *37* (9), 2028.

(20) Cheng, Y.; Samia, A. C.; Meyers, J. D.; Panagopoulos, I.; Fei, B.; Burda, C. Highly Efficient Drug Delivery with Gold Nanoparticle Vectors for in Vivo Photodynamic Therapy of Cancer. *J. Am. Chem. Soc.* **2008**, *130* (32), 10643–10647.

(21) Kim, Y.; Johnson, R. C.; Hupp, J. T. Gold Nanoparticle-Based Sensing of “Spectroscopically Silent” Heavy Metal Ions. *Nano Lett.* **2001**, *1* (4), 165–167.

(22) Kneipp, K.; Haka, A. S.; Kneipp, H.; Badizadegan, K.; Yoshizawa, N.; Boone, C.; Shafer-Peltier, K. E.; Motz, J. T.; Dasari, R. R.; Feld, M. S. Surface-Enhanced Raman Spectroscopy in Single Living Cells Using Gold Nanoparticles. *Appl. Spectrosc.* **2002**, *56* (2), 150–154.

(23) Xie, J.; Zhang, Q.; Lee, J. Y.; Wang, D. I. C. The Synthesis of SERS-Active Gold Nanoflower Tags for In Vivo Applications. *ACS Nano* **2008**, *2* (12), 2473–2480.

(24) Song, J.; Zhou, J.; Duan, H. Self-Assembled Plasmonic Vesicles of SERS-Encoded Amphiphilic Gold Nanoparticles for Cancer Cell Targeting and Traceable Intracellular Drug Delivery. *J. Am. Chem. Soc.* **2012**, *134* (32), 13458–13469.

(25) Grisel, R.; Weststrate, K. J.; Gluhoi, A.; Nieuwenhuys, B. E. Catalysis by Gold Nanoparticles. *Gold Bulletin* **2002**, *35* (2), 39–45.

(26) Daniel, M.-C.; Astruc, D. Gold Nanoparticles: Assembly, Supramolecular Chemistry, Quantum-Size-Related Properties, and Applications toward Biology, Catalysis, and Nanotechnology. *Chem. Rev.* **2004**, *104* (1), 293–346.

(27) Lu, Y.; Chen, W. Sub-Nanometre Sized Metal Clusters: From Synthetic Challenges to the Unique Property Discoveries. *Chem. Soc. Rev.* **2012**, *41* (9), 3594.

(28) Chakraborty, I.; Pradeep, T. Atomically Precise Clusters of Noble Metals: Emerging Link between Atoms and Nanoparticles. *Chem. Rev.* **2017**, *117* (12), 8208–8271.

(29) Yau, S. H.; Varnavski, O.; Goodson, T. An Ultrafast Look at Au Nanoclusters. *Acc. Chem. Res.* **2013**, *46* (7), 1506–1516.

(30) Wu, X.; He, X.; Wang, K.; Xie, C.; Zhou, B.; Qing, Z. Ultrasmall Near-Infrared Gold Nanoclusters for Tumor Fluorescence Imaging in Vivo. *Nanoscale* **2010**, *2* (10), 2244.

(31) Herzing, A. A.; Kiely, C. J.; Carley, A. F.; Landon, P.; Hutchings, G. J. Identification of Active Gold Nanoclusters on Iron Oxide Supports for CO Oxidation. *Science* **2008**, *321* (5894), 1331–1335.

(32) Du, X.; Jin, R. Atomically Precise Metal Nanoclusters for Catalysis. *ACS Nano* **2019**, *13* (7), 7383–7387.

(33) Sun, J.; Zhang, J.; Jin, Y. 11-Mercaptoundecanoic Acid Directed One-Pot Synthesis of Water-Soluble Fluorescent Gold Nanoclusters and Their Use as Probes for Sensitive and Selective Detection of Cr³⁺ and Cr⁶⁺. *J. Mater. Chem. C* **2013**, *1* (1), 138–143.

(34) Jeseentharani, V.; Pugazhenthiran, N.; Mathew, A.; Chakraborty, I.; Baksi, A.; Ghosh, J.; Jash, M.; Anjusree, G. S.; Deepak, T. G.; Nair, A. S.; Pradeep, T. Atomically Precise Noble Metal Clusters Harvest Visible Light to Produce Energy. *Chemistry Select* **2017**, *2* (4), 1454–1463.

(35) Chang, T.-K.; Cheng, T.-M.; Chu, H.-L.; Tan, S.-H.; Kuo, J.-C.; Hsu, P.-H.; Su, C.-Y.; Chen, H.-M.; Lee, C.-M.; Kuo, T.-R. Metabolic Mechanism Investigation of Antibacterial Active Cysteine-Conjugated Gold Nanoclusters in *Escherichia Coli*. *ACS Sustainable Chem. Eng.* **2019**, *7* (18), 15479–15486.

(36) Kurashige, W.; Niihori, Y.; Sharma, S.; Negishi, Y. Precise Synthesis, Functionalization and Application of Thiolate-Protected Gold Clusters. *Coord. Chem. Rev.* **2016**, *320–321*, 238–250.

(37) Chen, C.-H.; Lee, P.-W.; Tsao, Y.-H.; Lin, Z.-H. Utilization of Self-Powered Electrochemical Systems: Metallic Nanoparticle Synthesis and Lactate Detection. *Nano Energy* **2017**, *42*, 241–248.

(38) Liu, C.; Bard, A. J. Electrostatic Electrochemistry at Insulators. *Nat. Mater.* **2008**, *7* (6), 505–509.

(39) Baytekin, B.; Baytekin, H. T.; Grzybowski, B. A. What Really Drives Chemical Reactions on Contact Charged Surfaces? *J. Am. Chem. Soc.* **2012**, *134* (17), 7223–7226.

(40) Han, J.; Meng, X.; Lu, L.; Wang, Z. L.; Sun, C. Triboelectric Nanogenerators Powered Electrodepositing Tri-Functional Electrocatalysts for Water Splitting and Rechargeable Zinc-Air Battery: A Case of Pt Nanoclusters on NiFe-LDH Nanosheets. *Nano Energy* **2020**, *72*, 104669.

(41) Ceceri, K. *Make: Paper Inventions: Machines That Move, Drawings That Light Up, and Wearables and Structures You Can. Cut, Fold, and Roll*; Maker Media, Inc., 2015.

(42) Wang, Z. L.; Lin, L.; Chen, J.; Niu, S.; Zi, Y. Triboelectric Nanogenerator: Freestanding Triboelectric-Layer Mode. In *Triboelectric Nanogenerators*; Springer, 2016; pp 109–153.

(43) Qian, H.; Zhu, Y.; Jin, R. Size-Focusing Synthesis, Optical and Electrochemical Properties of Monodisperse Au₃₈ (SC₂H₄Ph)₂₄ Nanoclusters. *ACS Nano* **2009**, *3* (11), 3795–3803.

(44) Laaksonen, T.; Ahonen, P.; Johans, C.; Kontturi, K. Stability and Electrostatics of Mercaptoundecanoic Acid-Capped Gold Nanoparticles with Varying Counterion Size. *ChemPhysChem* **2006**, *7* (10), 2143–2149.

(45) Shivhare, A.; Wang, L.; Scott, R. W. J. Isolation of Carboxylic Acid-Protected Au₂₅ Clusters Using a Borohydride Purification Strategy. *Langmuir* **2015**, *31* (5), 1835–1841.

(46) Su, C. H.; Wu, P. L.; Yeh, C. S. PH Dependence of Interparticle Coupling for Gold Nanoparticle Assemblies Formation: Electrostatic Attraction and Hydrogen Bonding. *Bull. Chem. Soc. Jpn.* **2004**, *77* (1), 189–193.

(47) Chang, H.-C.; Chang, Y.-F.; Fan, N.-C.; Ho, J. A. Facile Preparation of High-Quantum-Yield Gold Nanoclusters: Application to Probing Mercuric Ions and Biothiols. *ACS Appl. Mater. Interfaces* **2014**, *6* (21), 18824–18831.